

# Water Resources Research

## RESEARCH ARTICLE

10.1029/2018WR024488

### Key Points:

- The formation of an isolated talik results in accelerated and potentially irreversible permafrost thaw
- A combination of field data and 1-D modeling is used to investigate the formation of isolated taliks
- Soil moisture, snow cover, and advection affect the formation and development of isolated taliks

### Supporting Information:

- Supporting Information S1

### Correspondence to:

É. G. Devoie,  
egdevoie@uwaterloo.ca

### Citation:



Devoie, E. G., Craig, J. R., Connon, R. F., & Quinton, W. L. (2019). Taliks: A tipping point in discontinuous permafrost degradation in peatlands. *Water Resources Research*, 55. <https://doi.org/10.1029/2018WR024488>

Received 27 NOV 2018

Accepted 3 NOV 2019

Accepted article online 12 NOV 2019

## Taliks: A Tipping Point in Discontinuous Permafrost Degradation in Peatlands

Élise G. Devoie<sup>1</sup> , James R. Craig<sup>1</sup> , Ryan F. Connon<sup>2</sup> , and William L. Quinton<sup>2</sup> 

<sup>1</sup>Department of Civil and Environmental Engineering, University of Waterloo, Waterloo, Ontario, Canada,

<sup>2</sup>Cold Regions Research Centre, Wilfrid Laurier University, Waterloo, Ontario, Canada

**Abstract** Taliks (perennially thawed soil in a permafrost environment) are generally found beneath water bodies or wetlands, and their development and evolution in other environments is poorly documented. Sustained isolated taliks between seasonally frozen surface soils and permafrost have been observed at the Scotty Creek Research Station in the discontinuous permafrost region of the Northwest Territories, Canada. These taliks have been expanding both vertically and laterally over the past decade of monitoring. The main controls on expansion are thought to be (1) the availability of energy, determined by incoming radiation and advective heat flux, (2) the ability to transfer this energy to the freezing/thawing front, determined by the thermal conductivity (soil properties and moisture content), and (3) the presence and thickness of the snowpack. These controls are investigated using data collected in the field to inform a 1-D coupled thermodynamic freeze-thaw and unsaturated flow model. The model was successfully used to represent observed thaw rates in different parts of the landscape. It is found that high soil moisture, deeper snowpacks, and warmer or faster advective flow rates all contribute to accelerated talik growth and subsequent permafrost degradation. Simulations show that slight perturbations of available energy or soil properties, such as an increase in average surface temperature of 0.5°C or a 1-cm change in snow water equivalent, can lead to talik formation, highlighting the vulnerability of this landscape to changes in climate or land cover.

## 1. Introduction

Permafrost regions are very sensitive to changes in climate, especially those classified as discontinuous or sporadic (Chasmer et al., 2011; Stendel & Christiansen, 2002; Zhao et al., 2010). Climate warming trends have been shown to cause permafrost degradation and loss, resulting in subsidence, wetland expansion, and landscape transition (Carpino et al., 2018; Rowland et al., 2010; Walvoord & Kurylyk, 2016). One of the mechanisms for permafrost degradation is cited as “active layer thickening,” driven by increases in mean annual air temperature, precipitation, and anthropogenic or natural land cover change or disturbance (Bonnaventure & Lamoureux, 2013; Shiklomanov et al., 2012). This process is indicative of permafrost degradation in continuous permafrost, where the active layer, or layer which freezes and thaws annually, is defined by the late summer maximum depth of thaw (Burn, 1998). However, in areas where permafrost is degrading, especially at the southern limit of permafrost, the active layer can either be determined by the depth of thaw or the late winter refreeze depth if a talik exists between the permafrost table and the active layer (Connon et al., 2018). In the second case, the depth of thaw exceeds the refreeze depth, leaving a perennially thawed region between the base of the active layer and the top of the degrading permafrost body.

Taliks are typically documented beneath or adjacent to water bodies such as wetlands or lakes (Bonnaventure & Lamoureux, 2013; Rowland et al., 2010; Woo, 2012), while the formation and evolution of shallow suprapermfrost taliks hydrologically isolated from wetland features over the winter season (hereafter referred to as isolated taliks) have received relatively little attention. Though briefly mentioned in field literature (e.g., Fisher et al., 2016), the factors controlling the formation of isolated taliks have not been thoroughly investigated in thermal modeling literature. A comprehensive review of current thermal models was completed by (Kurylyk, 2013); talik modeling was not mentioned. This omission is likely due in part to scale, where large-scale models do not resolve the relatively local process of talik formation, for example, Stendel and Christiansen (2002).

Freeze-thaw models based on analytic or semianalytic solutions of the Stefan problem (e.g., Hayashi et al., 2007; Hinzman et al., 1998; Krogh et al., 2017; Semenova et al., 2013; Woo et al., 2004; Zhang et al., 2003) are

unable to represent the three-tiered system (permafrost-talik-active layer) present in talik formation. These models may be inappropriate for modeling degrading permafrost at the local scale because they assume a linear temperature profile between the soil surface and the (single) freeze/thaw front. Existing continuum models (that do not assume a linear temperature profile; e.g., Daanen et al., 2008; Frampton et al., 2012; Jorgenson et al., 2010; Karra et al., 2014; McGuire et al., 2016; McKenzie & Siegel, 2007; Schaefer et al., 2009; Zhang et al., 2008) have thus far focused on longer-term lateral permafrost extent, water seepage, carbon storage, permafrost resilience, or other processes that do not distinguish controls on isolated talik formation or evolution in peatland environments.

The initiation of an isolated talik has been simulated by Frampton et al. (2012), Atchley et al. (2016), Yi et al. (2014), Endrizzi et al. (2014), Rawlins et al. (2013), Jafarov et al. (2018), Brown et al. (2015), and Walvoord et al. (2019), where controls on the active layer such as saturation, snow cover, shading, forest fire, and ponded water were quantified. These studies shed light on processes governing active layer thickness as defined by maximum thaw depth, but talik formation was not their focus. Nickolsky et al. (2016) simulated talik formation by the end of the century in the Alaskan North Slope under Representative Concentration Pathway 4.5 and 8.5 greenhouse gas scenarios, driven by changes in climate forcing, but moisture, snowpack, and incoming radiative effects were not distinguished. Evans and Ge (2017) simulated suprapermfrost layer thickening due only to increased mean annual air temperature in the aim of quantifying the effect of changes in frozen ground regimes on groundwater discharge.

The modeling efforts presented in this paper focus on the formation, evolution, and persistence of isolated taliks at the local scale. This work aims to build on existing work in discontinuous permafrost presented by Kurylyk et al. (2016) and Langford et al. (2019). Kurylyk et al. (2016) detail the lateral permafrost thaw and vertical thaw at the bottom boundary of permafrost bodies, while Langford et al. (2019) simulated a single peat plateau in the research basin. The detailed 3-D modeling work presented in these studies did not address vertical thaw at the top of a permafrost body or the formation of isolated taliks within permafrost plateaux.

It is proposed here that talik formation plays an important threshold-based (as defined by Grosse et al., 2016) thermodynamic role in the initiation of permafrost degradation at the interior of permafrost bodies in discontinuous permafrost regions and ultimately the hydrologic evolution of permafrost environments in the peatlands region of the southern Taiga Plains, Canada. The impacts of unsaturated soil conditions, moisture migration due to temperature and pressure gradients, lateral advection, and insulation due to variations in annual snowfall will be considered to explicitly identify drivers for talik formation. The subsequent permafrost degradation rate once a talik is formed is also presented for this ecosystem-protected permafrost environment. The objectives of this study are to (1) use a 1-D model to identify the conditions under which isolated taliks are likely to form, (2) assess the extent and controls on the rate of talik formation, and their consequences for permafrost evolution, and (3) evaluate the mechanisms by which talik formation can lead to a “tipping point” condition at which permafrost recovery becomes unlikely.

## 2. Study Site

Field studies were completed at the Scotty Creek Research Station (SCRS), located approximately 50 km south of Fort Simpson (MAAT  $-3.2^{\circ}\text{C}$ ) in discontinuous permafrost peatlands (described in Quinton et al., 2018). The site is ideal for the study of permafrost degradation because it includes permafrost in a variety of degradational stages including stable permafrost features, features with isolated and connected taliks, and permafrost-free wetland features (Connon et al., 2018). Here connected taliks refer to suprapermfrost taliks, which provide a perennial hydrologic flow pathway between adjacent thawed wetland features. The peat deposit in this study site ranges from 2 to 8 m in thickness and overlays clay, silt/clay, and low-permeability glacial till (Quinton et al., 2019). High permeability peat soils drain readily when the water table is below the ground surface, leaving a relatively dry insulating surface peat layer that preserves permafrost underlying peat plateaux (Quinton et al., 2009). Though insulated from high summer temperatures, the permafrost in this discontinuous permafrost site is warm, and a significant portion of it is within the zero curtain (undergoing phase change) as shown in Figure 1a. Peat plateaux are elevated above the surrounding permafrost-free wetlands due to the subsidence, which accompanies permafrost thaw and the loss of segregated ground ice. Plateaux have a relatively dry vadose zone, allowing them to support a black spruce canopy (Quinton et al., 2009). These plateaux are surrounded by two wetland types that dominate the landscape: collapse scar bogs

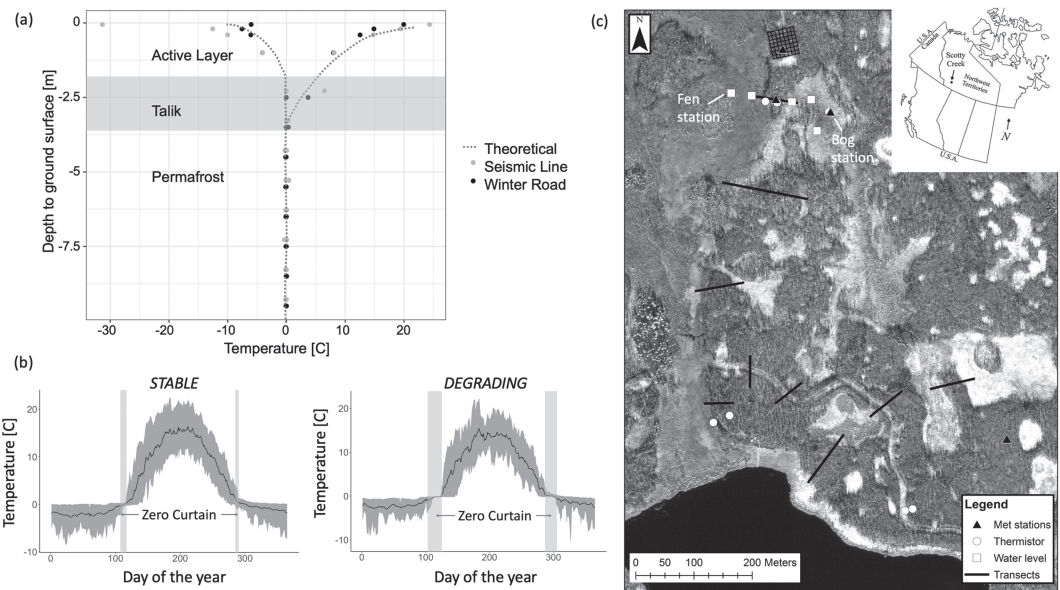


**Figure 1.** (a) Trumpet plot for ground temperatures measured at the SCRS, indicating maximum and minimum soil temperature at various depths. Dashed line illustrates the theoretical curve for this site. Data below the talik sit within the freezing point depression indicating permafrost undergoing phase change. (b) Range of soil temperatures measured on a stable peat plateau (*stable*) and a degrading peat plateau in the presence of a talik (*degrading*) at a depth of 5–10 cm below soil surface. Note that the moisture content increases with the formation of a talik, which is reflected in the duration of the zero-curtain periods. (c) Map of study site including frost table transects and grid, thermistor sites where soil temperature is measured in profile, water level recorders used to establish hydraulic gradient and subsurface temperature and meteorological stations monitoring a suite of climate variables including soil temperature and moisture described in section 3.1.

and poor fens that act mainly as water storage features and channel fens that act as the low-gradient routing feature in this flat, high-storage landscape (Gordon et al., 2016; Quinton et al., 2009).

In this landscape of ephemerally interconnected wetlands, lateral movement of water through the portions of the active layer that remain saturated most of the year is common and may help explain variability in permafrost degradation rates across the landscape (Connon et al., 2015). Peat plateaux adjacent to wetland features have been observed to degrade more quickly (both vertically and laterally) than plateaux with isolated taliks (Baltzer et al., 2014; McClymont et al., 2013); it is postulated that lateral advection through the talik plays a considerable role in determining the rate of permafrost degradation.

### 3. Methods

#### 3.1. Field Methods

This study focuses on the application of a 1-D vertical freeze/thaw model informed by boundary conditions and validation data collected at the SCRS to simulate a set of representative soil columns in a discontinuous permafrost environment. Temperature data were measured using Campbell Scientific CS107 or CS109 thermistors or Onset HOBO U12 four-channel thermistors and loggers. These were installed in depth profiles approximately every 5–20 cm from a depth of 5 to 50 cm, where the observation data used to generate boundary condition were measured at either a depth of 5 or 10 cm. Exact measurement depths and spacing varied across the measurement sites.

The permafrost that underlays peat plateaux in the landscape can be classified either as *degrading* or *stable*. The *degrading* boundary condition describes a plateau with an isolated talik that remains perennially thawed. The *stable* boundary condition describes a plateau in which the permafrost is not actively degrading, and there is complete refreeze of the active layer in most if not all years. Figure 1b shows surface temperature data collected in both conditions from which surface temperature boundary conditions were constructed.

Data to inform the mean and variance of the *stable* temperature boundary condition were collected at five different sites in the area of interest, three of which were located on the same permafrost plateau (Indicated as white circles on Figure 1c). Sites with moss and lichen ground cover were likewise represented; at least

three of the sites developed a talik before the end of the data record. Data up to 2 years preceding talik development were included in the data set used to generate boundary conditions for the stable condition. Talik formation was inferred if any one of the thermistors in the vertical profile did not drop below the zero curtain for five or more consecutive days. The data after the formation of a talik were combined with temperature data collected along an abandoned winter road (an anthropogenic cut line where permafrost has degraded visible in Figure 1c) to inform the *degrading* temperature boundary condition (those representing unsteady warming conditions) as observed in Figure 1b. Both field data time series included data gaps due to instrument malfunction but provided a roughly 10-year data record.

Deep soil temperature data were collected at two sites with degrading permafrost using RBR deep thermistors with 1-m spacing from 2 to 8 m below the ground surface white circles on Figure 1c. The temperature of lateral flow through a connected talik was assigned based on the average daily temperature at 40–50 cm below the ground surface in wetlands in the landscape. Subsurface temperature data for a bog were only available for a single sampling location (labeled “bog station” in Figure 1c), though these data were consistent over the more than 10-year period of record. Similar data were available for a channel fen (the “fen station”), though the period of record was only 4 years and contained several data gaps. Temperature data collected at three other locations in a fen using HOBO U20 pressure transducers and temperature loggers were consistent with this shorter data series. Lateral advective flow rates ( $q_y$ ) were estimated based on available hydraulic gradients measured using sets of HOBO U20 pressure transducers installed in adjacent features (shown as white circles in Figure 1a). Soil moisture boundary conditions were based on measured moisture content at a depth of 20 cm using Campbell Scientific CS 615 and Campbell Scientific CS 616 water content reflectometers located at meteorological station indicated as black triangles in Figure 1a. Probes were calibrated according to the manual using soil samples collected at the SCRS. Model parameters such as saturated hydraulic conductivity, porosity, thermal conductivity, field capacity, and others listed in Table S1 of the supporting information were fixed at representative values, either measured in the field, or found in literature (e.g., thermal conductivity of peat), without model calibration.

Validation data included temperature data measured in the same locations as above, but at a depth of 50 cm, as well as frost table measurements along nine transects and one grid, (black lines and grid in Figure 1c) documenting lateral and vertical permafrost thaw rates. Monitoring points were located along transects traversing permafrost plateaux and intersecting the border of bogs and fens in order to contrast permafrost degradation adjacent to different wetlands. The transects were established in 2011, and permafrost degradation along these transects has been measured annually since 2015, as described in detail by Connon et al. (2018).

In typical stable permafrost environments where the ground annually refreezes to the permafrost table, active layer depth can be measured at the end of the thaw season, but taliks are prevalent at the SCRS, resulting in an active layer depth that can only be determined by knowing the (hard to measure) refreeze depth. In the instance of a talik, the active layer is therefore measured in early spring before ground thaw begins by drilling through the frozen soil to find the base of the frozen layer as detailed in Connon et al. (2018).

### 3.2. Modeling Methods

Two coupled differential equations are used here to represent the problem of heat and water transport in freezing soils. These equations are solved in one dimension using an iterative Crank-Nicolson finite volume solver. Water movement is governed by the unsaturated Richards' equation (represented in mixed form here, similar to Celia et al., 1990):

$$\left( \frac{\partial \theta_l}{\partial \psi} + S_s \right) \frac{\partial \psi}{\partial t} + \left( \frac{\rho_i}{\rho_l} \theta_i + \theta_l \right) \frac{\partial F(T)}{\partial t} = \frac{\partial}{\partial z} \left( K(\psi, T) \frac{\partial \psi(z, T, \theta)}{\partial z} \right) \quad (1)$$

where  $\theta$  (–) represents water saturation,  $\psi$  (m) is soil matric potential,  $S_s$  ( $\text{m}^{-1}$ ) is specific storage,  $t$  (s) is time,  $\rho$  ( $\text{kg}/\text{m}^3$ ) is density,  $F$  (–) is the temperature-dependant ice fraction,  $T$  ( $^{\circ}\text{C}$ ) is temperature,  $z$  (m) is vertical distance, and  $K$  (m/s) is hydraulic conductivity. The hydraulic conductivity is given using the van Genuchten model with peat-specific parameters (van Genuchten, 1980). The hydraulic conductivity is modified by an empirical relationship describing the impedance of ice content to water movement through the partially saturated soil, as presented by Kurylyk (2013). The subscripts  $l$  and  $i$  refer to liquid water and ice phases respectively. The less common term  $\left( \frac{\rho_i}{\rho_l} \theta_i + \theta_l \right) \frac{\partial F(T)}{\partial t}$  on the left-hand side is a source/sink term arising from the inclusion of phase change. Vapor flux is not included in this model; Putkonen (1998) deemed

it unimportant (especially in wet soils) as compared to the other processes occurring in an unsaturated 1-D freezing or thawing soil column. The main role of vapor flux is to deliver water to the freezing front, which is accomplished instead by the Clausius-Clapeyron (CC) relation (Karra et al., 2014). The CC relation is included in the  $\frac{\partial \theta_l}{\partial \psi}$  term in equation (1) when the temperature is in the freezing range, assumed to be 0 to  $-0.05^\circ\text{C}$  (equation (2)). This equation is very similar to the form of the Clausius relationship presented in Kurylyk (2013). The terms  $g$ ,  $L$ , and  $\Delta\rho^{-1}$  refer to gravity ( $\text{m/s}^2$ ), the latent heat of fusion of water ( $\text{J/kg}$ ), and the change in specific volume associated with the phase change ( $\text{m}^3/\text{kg}$ ), respectively.

$$\frac{\partial \theta_l}{\partial \psi} = \frac{d\theta_l}{d\psi} \frac{d\psi}{dz} = \frac{d\theta_l}{d\psi} \left( 1 - \frac{\partial \psi(\theta)}{\partial z} + \frac{1}{\rho g} \frac{L}{T \Delta \rho^{-1}} \frac{\partial T}{\partial z} \right) \quad (2)$$

Heat transport in the porous media is governed by

$$\left[ c\rho + L \frac{dF}{dT} \rho \eta \theta \right] \frac{\partial T}{\partial t} = \left( \frac{\partial}{\partial z} \left( \lambda_b \frac{\partial T}{\partial z} \right) - c_l \rho_l \frac{\partial q_z T}{\partial z} \right) + q_y \rho_w c_w (T_{in} - T) \quad (3)$$

in which the parameters  $c$  ( $\text{J}\cdot\text{kg}^{-1}\cdot^\circ\text{C}^{-1}$ ),  $\eta$  ( $-$ ),  $\lambda_b$  ( $\text{J}\cdot\text{m}^{-1}\cdot\text{s}^{-1}\cdot^\circ\text{C}^{-1}$ ), and  $q$  ( $\text{m/s}$ ) refer to bulk heat capacity, porosity, bulk thermal conductivity, and flow rate of liquid water, respectively. The subscripts  $z$  ( $\text{m}$ ) and  $y$  ( $\text{m}$ ) refer to the vertical and horizontal directions, and  $T_{in}$  ( $^\circ\text{C}$ ) is the temperature of water laterally entering the soil column driving advection. Note that water may be supplied laterally to the column via the final  $q_y$  term, with the flux given by  $q_y = -K(\psi, T) \frac{\partial h}{\partial y}$ , where the gradient is fixed for each simulation and  $K$  values reflect the impedance due to ice content. This term is used only when the soil column contains a talik connected to a wetland feature. The inclusion of this source term allows the 1-D vertical model to represent lateral water movement in short-term simulations of permafrost evolution. This method is not appropriate for long-term change detection where lateral permafrost thaw is expected.

These equations have individually been solved elsewhere, and the uncoupled formulations (i.e., unfrozen Richards' and saturated conductive heat transport) were separately benchmarked against results from Kurylyk et al. (2014) and Celia et al. (1990). No existing analytical models are available to benchmark the coupled set of equations. The relationships are coupled using operator splitting, first solving the unsaturated Richard's equation and then the heat transport equation in each time step, using an approach similar to Harlan (1973). The specific storage  $S_s$  is dependent on ice content,  $\theta_i$ , which is determined from the temperature  $T$ , as is the hydraulic conductivity,  $K$ . Moisture migration due to temperature gradients near the freezing temperature is allowed using the CC relationship. The inclusion of this process changed model predictions less than 1% in saturated conditions but reduced model stability and increased computation time. Bulk parameters are calculated based on the ice/water/air fractions in the soil matrix, where the heat capacity ( $c$ ) and density ( $\rho$ ) are calculated using the volumetrically weighted arithmetic mean of saturation values determined by the unsaturated Richards' equation, and the thermal conductivity  $\lambda_b$  is calculated using a volumetrically weighted geometric mean, as suggested by Kurylyk et al. (2014). The physical properties of the assumed soil column are homogenous, except those which depend on the water or ice saturation of the profile, which are allowed to vary with soil water or ice content. The omission of depth-dependant parameters most affects the hydraulic conductivity in the top 0.3 m of the soil profile, as the other modeled parameters are relatively constant with depth (Quinton et al., 2008). This may speed the equilibration time of the profile when subject to specified water flux conditions due to higher hydraulic conductivity near the surface but is not expected to drastically affect model results and still permits the comparison of various drivers of permafrost degradation.

As seen in Figure 2, the soil column is discretized into 2-cm elements for all simulations. For simulations where the soil column is saturated (i.e., not those investigating unsaturated conditions), a 0.48-hr time step is used. In unsaturated conditions this is refined to 0.24 hr to ensure convergence and is further refined when moisture migration due to temperature gradients is included to 0.12 hr. In all cases, the thermal operator converged at each time step. In the unsaturated case with moisture migration due to temperature gradients, the moisture operator (equation (1)) failed to converge no more than 0.5% of the simulation time. This lack of convergence occurred in the shoulder seasons, when the hydraulic conductivity is modified by ice content and very sharp gradients due to relatively rapid movement of the freeze/thaw front were observed as see in Figure 1b.

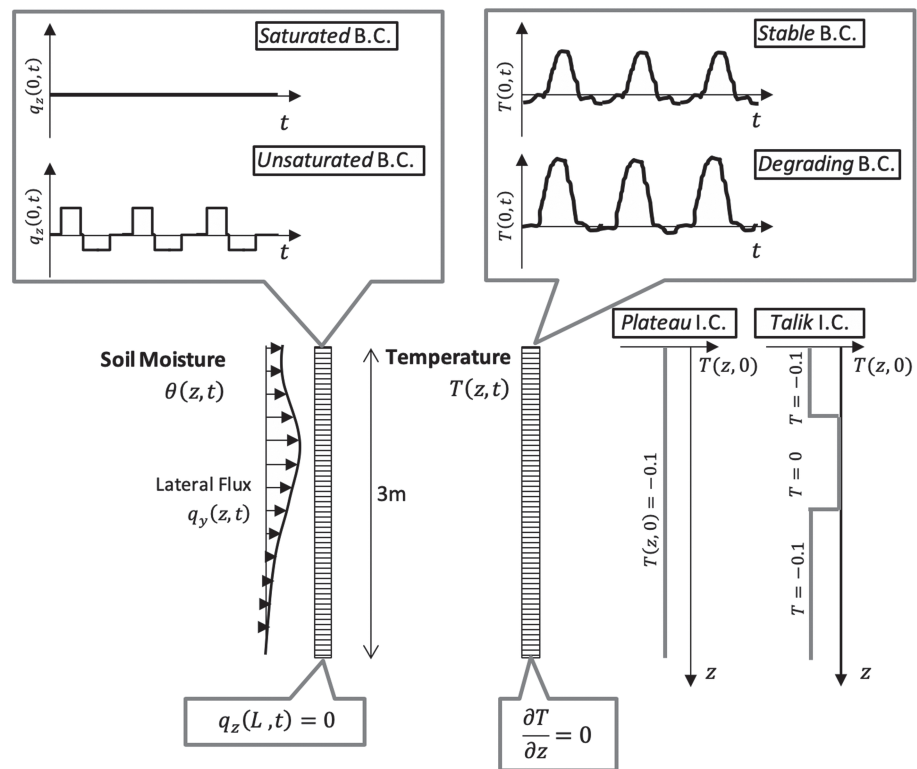


**Figure 2.** Model domain showing boundary conditions and initial conditions for various simulation experiments for both soil moisture and thermal relations.

### 3.3. Boundary and Initial Conditions

As a peatland, the study site maintains a water table near the ground surface. The water table is found within the top 0–30 cm of the soil profile in the wetlands and in depressions atop peat plateaux. The sloping edges of the peat plateaux are able to drain to adjacent wetlands, and the interior of the plateau can drain to internal depressions. In these locations, the water table is often found just above the frost table at a depth of 30–80 cm below the ground surface depending on time of year. A depth of –50 cm is representative of a well-drained area for most of the thawing season.

The surface boundary condition for the Richards' equation used here is a specified flux condition. Saturated conditions are simulated with a no-flow surface condition imposed on an initially saturated soil column. For unsaturated conditions, the average depth to water table of –50 cm on peat plateaux is used as an initial condition. A constant specified flux condition derived from water level records consists of the removal of 10 cm of water between mid-May and the end of June and the addition of the same amount of water between mid-August and the end of September. A no-flow condition is imposed at the base of the soil column, where it is assumed that permafrost is always present. A diagram of the model setup including both thermal and water content initial and boundary conditions is included in Figure 2.

Thermal boundary conditions are given by the ground surface temperature as modified by the presence of the snowpack, generated using a seasonal autoregressive moving average model following the method outline by Hipel and McLeod (1994) constructed using soil temperatures collected in the field. This allowed to generate multiple independent temperature boundary conditions with the same statistical properties as the collected field data. It was necessary to use a continuous data set from the same field site to appropriately capture the data covariance. For the *stable* case, only a 4-year time series was available for building the autoregressive model. In the *degrading* case, a longer 10-year data set was available, though it had a data gap of approximately 6 months. Therefore, only a 4-year subset was used to generate the autoregressive model, while the entire series was tested for stationarity. Both data sets were tested for stationarity: It was found that a stationary model was sufficient for *stable* permafrost, while a linear trend of +0.055°C/year was apparent in the deseasonalized data for the *degrading* case. This positive trend was applied when generating

ensemble temperature data for this boundary condition. Boundary conditions realizations for either 5- or 10-year simulations were sampled from the *stable* and *degrading* models reproducing seasonal trends and data variance observed in the field while incorporating interannual variability. The bottom thermal boundary condition is a zero heat flux condition. Field data show that the permafrost is effectively isothermal at 0°C to a depth of 8 m, and simulations have a maximum vertical depth of 3 m, so the geothermal gradient (of approximately 0.08 W/m<sup>2</sup>; McClymont et al., 2013) is neglected; see Figure 1a.

Heat flux at the ground surface is a clear direct driver of permafrost degradation (e.g., Walvoord et al., 2019). Changes in tree canopy, surface albedo, and ground cover contribute to modified ground heat flux (Quinton et al., 2018). This change is incorporated into model simulations as an increase in soil surface temperature in the summer. It would not be expected that the duration of the summer and winter season or the overwinter temperatures should be affected due to a change in canopy, unless there are changes to the snowpack due to interception. In the winter season, the ground heat flux is controlled by snow accumulation. Snow cover, and interannual variability in snow cover, has important implications for the ground thermal regime. End of season snow surveys are conducted annually across all landcover types at the SCRS providing an estimate of snow water equivalent (SWE), or total water stored on the landscape in the form of snow.

Once a talik exists in the soil profile, it is possible for it to connect adjacent wetland features. In the case of a connected talik, lateral advection through the talik is parameterized by treating throughflow as a distributed source/sink term in the 1-D energy balance. The lateral hydraulic gradient contributing to  $q_y$  in equation (3) is specified as 0.002 in the case of a connection to a collapse scar wetland and 0.007 in the case of a channel fen. The gradients are selected based on water level data collected in the field. Actual field data from connected talik features show variations and even reversals in hydraulic gradient over the year, but for simplicity these are omitted in favor of the average observed differences between wetland types. The range of inflow temperatures was derived from measurements in a collapse scar wetland and a channel fen at a depth of 50 cm below the ground surface. Sensitivity to changes in gradient are computed to put this assumption into context. For simplicity, this study neglects any freezing point depression and assumes phase change occurs between 0 and −0.05°C, while data collected at the field site indicate a very small freezing point depression.

Two sets of initial temperature conditions are used in model simulations: a *plateau* condition and a *talik* condition. These conditions describe (generalized) field observations of midwinter soil temperatures on a stable peat plateau and a plateau with an isolated talik, respectively. The *plateau* initial temperature profile is a uniformly frozen soil column at a constant temperature of −0.1°C. The *talik* condition is initialized to the same temperature as the *plateau* condition, except from a depth of 0.75 to 1.5 m, which is initialized at a temperature of 0°C and zero ice content as seen in Figure 2.

## 4. Results and Discussion

### 4.1. Model Evaluation

After the model was successfully benchmarked against both thermal and water content models from literature (Celia et al., 1990; Kurylyk et al., 2014) (see supporting information), the performance of the model was evaluated in relation to soil temperatures and refreeze depths measured at the SCRS. This ensured that the governing processes in this field site were represented adequately, and the approximated depth-homogenized soil properties were appropriate.

#### 4.1.1. Soil Temperature

The model was first tested by comparing modeled and measured temperatures at depth (40–50 cm below ground). *Stable* boundary conditions were applied to an unsaturated *plateau* initial condition with water table initially 50 cm below the soil surface to best represent a permafrost plateau. All model simulations are summarized in Table S2 of the supporting information. A contour plot of temperature evolution for the stable peat plateau boundary condition, as well as a comparison of modeled and measured temperatures at approximately 45 cm is shown in Figures 3a and 3b. These results were obtained without model calibration. Modeled soil temperatures adequately represent the zero-curtain period both during spring melt and winter freeze up. Measured data at all depths have high variability relative to modeled data because they are aggregated from data collected at five different sites over approximately 10 years (with data gaps) including intersite variability, while simulated boundary conditions are constructed from data collected at a single instrumented site.

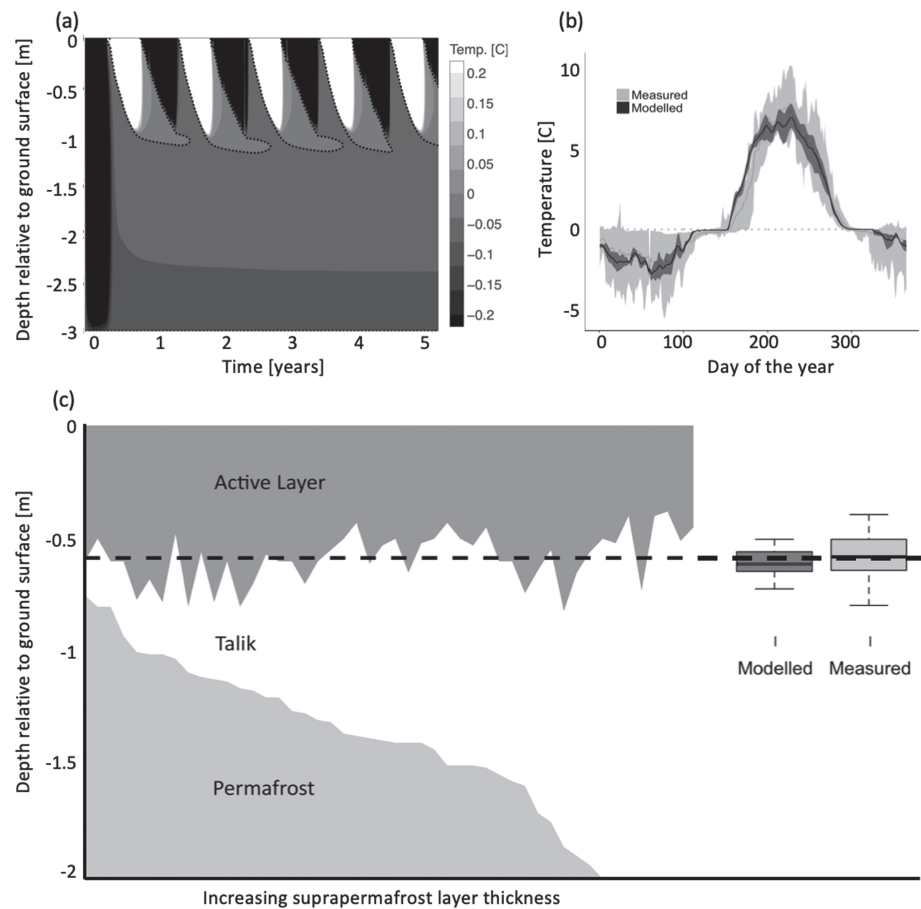


**Figure 3.** Modeled stable permafrost plateau. (a) shows freeze-thaw cycles over 5-year simulation. (b) Range of measured and modeled temperatures at 40 cm below ground surface for the soil column. (c) Measured refreeze and underlying permafrost is shown on the left, sorted by increasing depth to permafrost ( $n = 48$ ). Dashed line indicates average refreeze (over a talik). Box and whisker plots indicate the measured and modeled variance in active layer (refreeze) depth ( $n = 12$ ).

#### 4.1.2. Refreeze Depth

Though there is good agreement between modeled and measured soil temperature at depth, latent heat represents a large fraction of the system's energy storage and transfer (Hayashi et al., 2007), so the depth of freeze/thaw is also compared to field measurements of active layer (Figure 3c). Field measurements of maximum thaw depth in the absence of a talik reported  $59 \pm 4.5$  cm ( $n = 106$ ) and  $60 \pm 4.1$  cm ( $n = 99$ ) in 2016 and 2017, respectively, while the maximum refreeze with a talik was  $58 \pm 12.2$  cm ( $n = 120$ ) and  $59 \pm 11.5$  cm ( $n = 48$ ) in 2017 and 2018, respectively. Numbers in parentheses indicate the number of point measurements. Modeled soil columns with a talik align well with the measured value of refreeze over a talik:  $61 \pm 6.7$  cm ( $n = 12$ ), while simulations without a talik very slightly underestimate the maximum thaw depth:  $56 \pm 10.5$  cm ( $n = 15$ ). Given the agreement between modeled and measured soil temperatures and active layer depths, the model was deemed sufficient for the evaluation of controls on talik formation.

The benchmarked and verified model was used to (1) assess the relative influence of controls on isolated talik formation from a continuous permafrost state (section 4.2) and (2) determine how these factors affect permafrost degradation rates once a talik is formed (section 4.3).

#### 4.2. Controls on Talik Formation

Conditions favorable to talik formation on a permafrost plateau are identified based on the (a) soil moisture, (b) soil surface temperature, and (c) snow cover. All simulations of talik formation were subject to the *plateau* initial condition and (unless otherwise stated) the *stable* boundary condition. Average snow conditions for the study site (115 mm SWE) are used in all simulations except those testing the impact of changes in SWE.

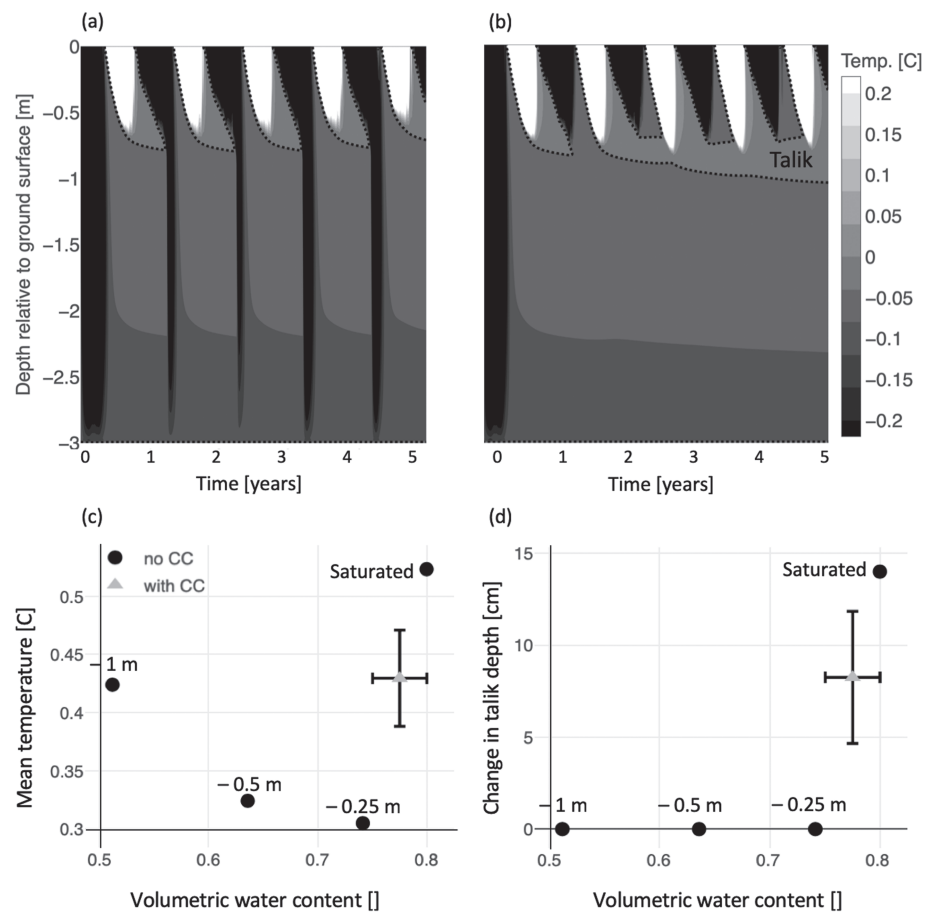


**Figure 4.** Soil temperatures over 5-year simulation with *stable* boundary condition for (a) data-driven unsaturated soil conditions with initial water table 25 cm from soil surface and (b) hypothetical saturated conditions. Dashed line indicates the maximum thaw contour. Panels (c) and (d) present the respective response in mean temperature of near-surface soil and talik thickness to changes in soil moisture (labeled by initial position of the water table below the ground surface).

#### 4.2.1. Unsaturated Soil Conditions

To determine the impact of different soil moisture conditions on talik formation, a modeled saturated soil column was compared to three unsaturated columns. For the unsaturated cases, the water table was initially set to a depth of 0.25, 0.5, and 1 m, and then subject to a specified flux boundary condition, with and without moisture migration due to temperature gradients.

Figure 4 compares the unsaturated (a) and saturated (b) cases. It can be seen by examining the  $0^{\circ}\text{C}$  isotherm that in the unsaturated case there is complete refreeze of the soil column each winter, while the freezing front penetrates the soil column further than the thawing front. This can be compared to the saturated case in Figure 4b, in which a talik forms. The unsaturated surface condition in the summer plays a key role in insulating the permafrost, protecting it from degradation evident in Figure 4b as the expanding region in the zero curtain (between 0 and  $-0.05^{\circ}\text{C}$ ).

The response of the mean temperature in the top 1 m of soil, and talik thickness to changes in soil moisture are presented in Figures 4c and 4d. The mean temperature and the volumetric water content are evaluated over the course of the entire 5-year simulation, while the maximum talik thickness is evaluated in the final winter of the simulation. Part (c) of the figure shows that as the moisture content increases, the mean annual soil temperature decreases, likely because more energy is required to heat a wetter soil profile. As the water table moves further from the soil surface, it becomes more difficult to draw the water to the freezing front, insulating the soil column overwinter. The saturated case is drastically different from the unsaturated case because it is not subject to the seasonal water flux at the soil surface. This flux plays an important role in cooling the profile as it increases the thermal conductivity over winter and decreases it during the warmest part

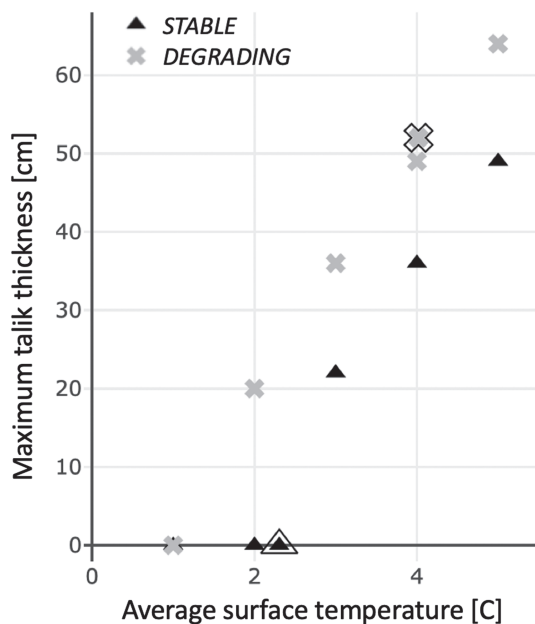


**Figure 5.** Response of talik thickness to changes in mean annual soil surface temperature. Temperature profile derived from the *stable* boundary condition shown in triangles, and *degrading* boundary condition in crosses. The original boundary condition (before summer temperature modification) is outlined in black.

of the summer. The inclusion of the CC relation in the simulations (gray triangles) obfuscates the moisture effects because the temperature gradient draws water to the soil surface, bringing the upper soil near saturation. With the CC relation, the applied boundary and initial conditions are not impactful on simulation results, which are shown as an average with standard deviation.

Only the saturated soil column develops a talik without the addition of moisture migration to the freezing front, and though the least saturated case has a warm mean annual temperature, it does not have sufficient heat capacity to offset the overwinter freezing of the soil column. The decreased soil moisture also leads to very low thermal conductivity, limiting the ability of this heat to penetrate the soil column and cause permafrost thaw. The active layer in these simulations is deeper but is not saturated and stores no more energy than the saturated conditions. In all cases involving the CC relation, a talik was formed. This is thought to be due to the near-saturated conditions induced in the near-surface during both freezing and thawing. The migration of moisture to the thawing front overcomes the imposed summer drying and winter wetting, leading to near-saturated conditions. However, the simulations without the CC relation are consistent with moisture conditions observed in the field and should therefore be considered when understanding the impact of soil moisture on talik formation.

In the field it is thought that taliks are associated with increased soil moisture, and differences in soil moisture are the driving control on differentiating land cover types, where the presence of (dry) lichen indicates higher permafrost stability, as reported by Grant et al. (2017), O'Donnell

et al. (2009), and many others. These simulations seem to confirm this field observation. Other modeling studies have found that soil moisture is less impactful on active layer evolution and talik formation when compared to changes in snowfall, but they do not include the observed seasonality in soil moisture leading to dry summer conditions and wet winter conditions (Atchley et al., 2015). The inclusion of this seasonality alleviates the competing processes of increasing thermal conductivity due to increasing moisture content, with a concomitant increase in latent heat required to fully freeze/thaw the soil column observed in other modeling studies (Atchley et al., 2015).

#### 4.2.2. Temperature

Summer soil surface temperatures were altered to reproduce changes in heat flux into the ground representative of differences in incoming radiation or surface albedo. Both the *stable* and *degrading* boundary conditions were considered. Results are reported in terms of annual mean surface temperature. Figure 5 shows the thickness of talik formed due to changes in mean annual surface temperature. Both responses are near linear, with the *degrading* condition forming a notably thicker talik at cooler temperatures. The shape of the temperature profile drives the *degrading* condition to store more heat despite the same mean annual temperature in both simulations. The *degrading* condition differs most prominently from the *stable* condition in that the zero-curtain period is longer. This delay in freezing and thawing may lead to a net energy gain to the system, where the zero-curtain does not provide a temperature gradient sufficient to freeze the soil in the fall, while the (shorter) spring zero-curtain period occurs earlier than in the *stable* case, leaving the summer thaw season approximately the same length in both cases.

#### 4.2.3. Snow Cover

It is widely understood that snow is a highly effective insulator due to its large (60–90%) air volume. When there is an early or thicker than usual snowpack, the soil temperatures are warmer than usual (Woo, 2012). Though somewhat data limited at this field site (established in 2006), Figure 6c shows that this relationship holds true at the SCRS. The relationship between SWE and soil temperature was used to test the impacts of increased snowfall by uniformly increasing the average overwinter temperature for the *stable* condition where the empirical relation from Figure 6c was used to determine the impact on winter soil temperatures. An increase in soil surface temperature derived from the linear relationship between SWE and overwinter soil temperature (Figure 6c) was applied to only the first winter (Figure 6a) and then the first

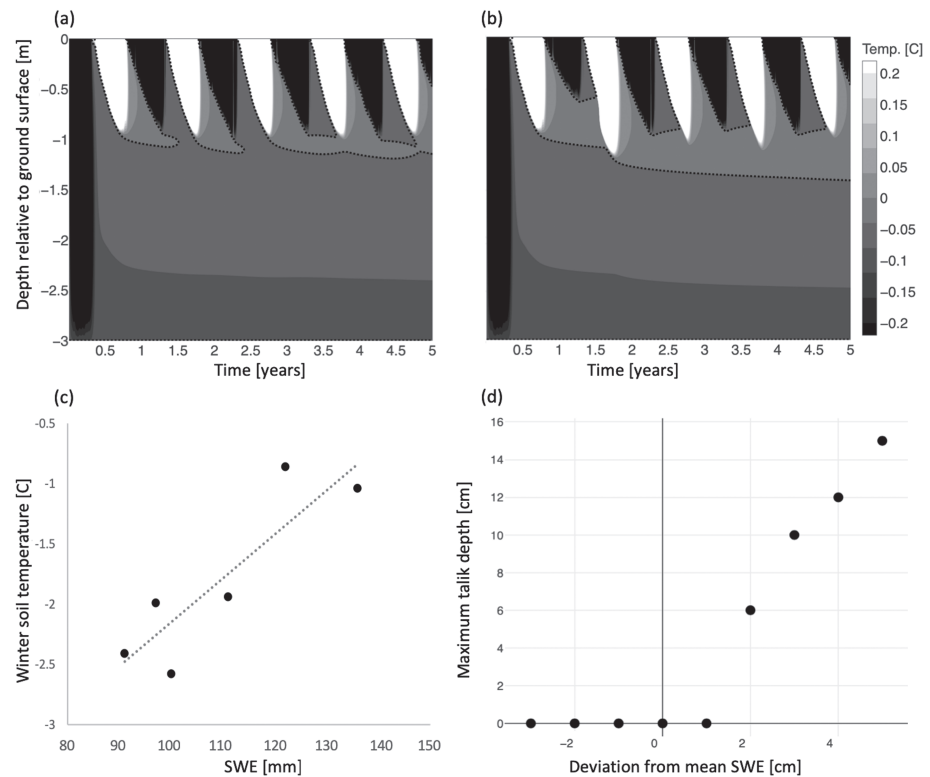


**Figure 6.** Impact of snow accumulation on soil temperatures. (a) One high (SWE = 125 mm) snow winter. (b) Two consecutive high snow winters. (c) Average winter (November–April) ground temperature at 5–10 cm in relation to maximum snow accumulation.  $R^2 = 0.77$ . (d) Modeled talik thickness response to changes in SWE in Winter 2.

and second winter (Figure 6b). Though there is no immediate talik development in the first case, it should be noted that the talik formed in the fourth winter is actually due to the additional energy stored in the soil profile from the first high snow winter, as without it, the simulation results in Figure 3a. The second case clearly confirms that increased snow cover can be a trigger for talik formation. These results were also found in the study by Atchley et al. (2015) and Atchley et al. (2016), in which it was shown that increased snow cover could lead to talik formation near Barrow, AK. Similarly to that study, increased snow resulted in an extension of the zero-curtain period, and a decrease in the maximum depth reached by the freezing front in high snow years (Atchley et al., 2015). Some climate change scenarios predict higher snowfall in the study region (Solomon et al., 2007). Snow depth may also be increased locally by talik formation, which leads to the development of local depressions where snow will preferentially accumulate, a forward feedback mechanism. These depressions and accompanying increased snow depth have been observed at the SCRS. This is similar to sites with shrub development, where Jafarov et al. (2018) have shown that the preferential snow accumulation within shrub patches can lead to the formation of isolated taliks that evolve from closed taliks to through taliks.

The opposite process, in which low-snow years can reverse the formation of a talik, is less likely. A decrease in SWE of equal magnitude to the initial increase is required to reverse the formation of a talik. Similarly to other regions in which the overwinter snowpack undergoes transformations such as sublimation and redistribution, the statistical distribution of annual SWE near the study site is skewed. It shows a tail toward high snow years, and a higher probability of just below average low-snow years (Shook et al., 2015). Therefore, it is unlikely to see an equal magnitude SWE deficit.

The sensitivity of talik formation to snow cover was tested by modifying the *stable* case with winter temperatures shifted resulting in a mean surface temperature of 2°C as the original saturated *stable* condition resulted in talik formation with no change in SWE. Figure 6d indicates the necessary deviation from mean SWE (temperature shift applied only in the second winter) to form a talik is approximately 2 cm.

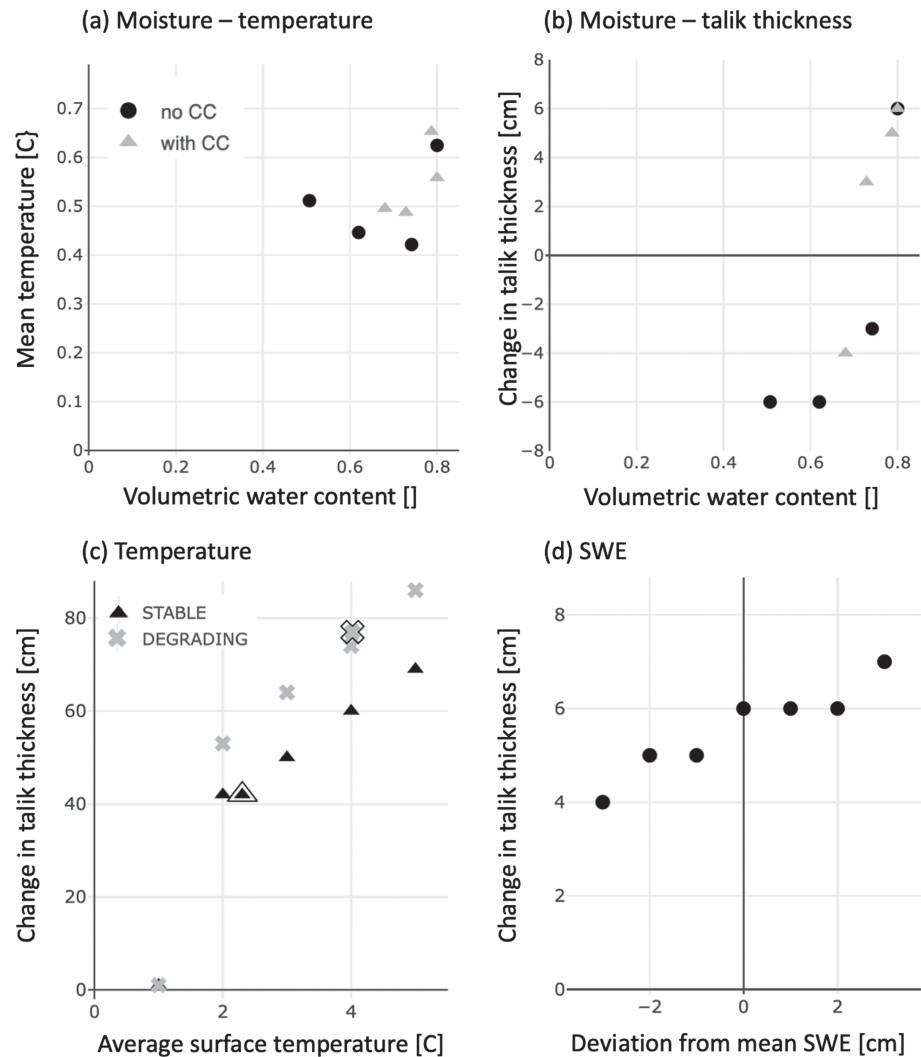


**Figure 7.** (a) Sensitivity of average soil temperature of top 1 m of soil profile (only in the case of soil moisture). Change in talik thickness due to (b) soil moisture, (c) average surface temperature, and (d) changes in SWE for *talik* initial condition.

### 4.3. Talik Evolution

Soil moisture, temperature, and snowfall conditions have been identified under which taliks are formed, initiating permafrost degradation. Once a talik is present in the soil column, field observations indicate that it is likely that permafrost will continue to degrade. The sensitivity of this permafrost degradation to the same conditions studied above is presented here. These results are extended to include the impacts of advection through the newly formed lateral flow path. Simulations in the following sections are run with the *talik* initial condition and (unless otherwise specified) the *stable* boundary condition so as to be directly comparable to the simulations of talik formation. Average snow conditions for the study site are used in all simulations except those testing the impact of changes in SWE.

#### 4.3.1. Soil Moisture

The impact of soil moisture on average temperature in the top 1 m of the soil column is very similar in the *talik* condition and the *plateau* condition, especially when the CC relation is not applied (Figure 7a). With a talik, there is less temperature-driven movement of water in near surface, resulting in similar trends in temperature as the case neglecting the CC relation. In all cases, the mean temperature is higher than without a talik.

The impact of unsaturated conditions on the thickness of the talik is quite remarkable. All unsaturated conditions without the CC relation and the condition with lowest soil moisture including the CC relation

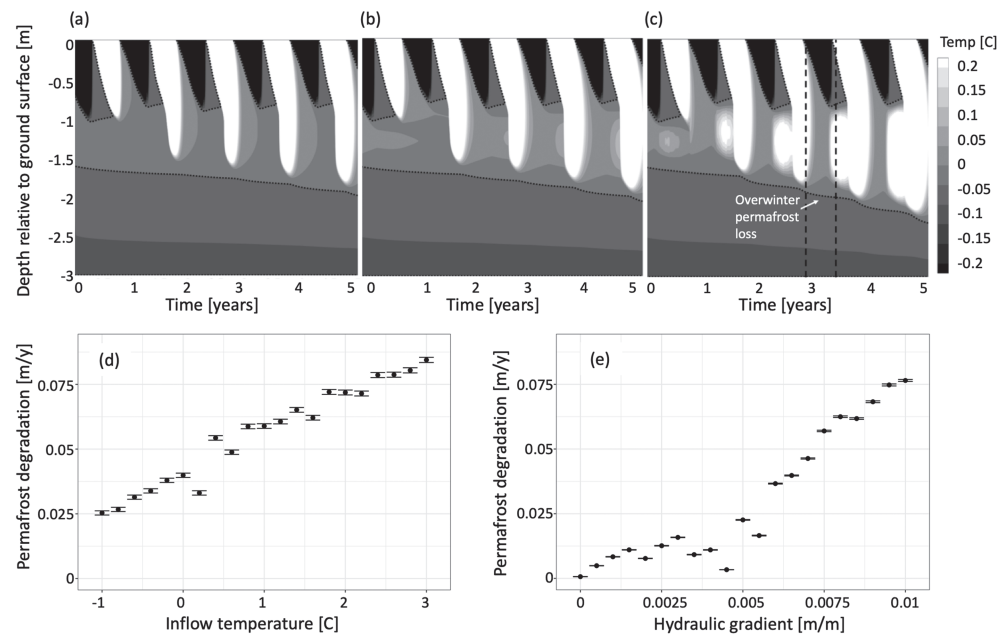


**Figure 8.** Soil temperatures as a result of advection representative of (a) an isolated talik, (b) a connected talik adjacent to a bog, or (c) a fen. Rate of vertical permafrost degradation determined by temperature (d) for a constant gradient of  $7 \times 10^{-3}$ , and hydraulic gradient (e) where the inflow temperature is unaltered from field measurements

resulted in talik thinning and evidence of permafrost recovery. This contrasts the saturated conditions (and near-saturated conditions with temperature-driven moisture migration) in which the talik thickens over the 5-year simulation.

#### 4.3.2. Temperature

An increase in talik thickness was found in the case initialized with a talik for all surface temperatures above  $2^{\circ}\text{C}$  (Figure 7c). A decrease in mean annual temperature up to  $1^{\circ}\text{C}$  did not seem to lead to permafrost recovery as the talik thickness remained constant. Simulated increased summer temperatures result in faster permafrost degradation beneath a preexisting talik than over a plateau forming a talik.

#### 4.3.3. Snow

The relationship between snowfall and permafrost degradation is very similar before and after the formation of a talik; that is, small increases in SWE help to insulate the ground leading to increased talik thickness. Though the trend remains the same, an increase in talik thickness is observed in all cases tested, while in the simulation started with the *plateau* condition only showed talik development after a SWE increase of 20 mm (Figure 7d). Even under low-snow conditions, the talik in the profile is observed to thicken by 4 cm over the course of the simulation, with no evidence of permafrost recovery.

#### 4.4. Advection

Here, three hypothetical soil columns with the *talik* initial condition and *degrading* boundary condition are modeled to examine the role of advection: (1) an isolated talik (without advection), (2) a connected talik with a hydrological connection to a collapse scar wetland, and (3) a connected talik with a hydrological connection to a channel fen. A hydraulic gradient of 0.002 was applied in the case of the bog and 0.007 in the case of a fen, while the isolated talik was not subjected to any lateral flow. Figures 8a–8c show that although all three simulations result in permafrost degradation, advection accelerates thaw rates and increases the sensible heat stored in the soil profile. As reported by Sjöberg et al. (2016), the abrupt changes in temperature of water flowing through the soil column in a fen observed at the SCRS can have significant impacts on thaw rates because of the high thermal gradients induced. In both cases including advection it is apparent that there is overwinter permafrost thaw in connected taliks adjacent to wetlands, which is not present without advection (see annotations in Figure 8c). This overwinter degradation has been observed in the field in a talik connecting a fen on one side to a bog on the other. Overwinter permafrost degradation can be seen as a tipping point, where permafrost recovery is highly implausible as degradation occurs year-round.

No plausible conditions could be identified through modeling that led to permafrost recovery in this case, nor have there been any instances of permafrost recovery observed under these conditions in the field.

The inclusion of plausible advection rates roughly doubles the modeled permafrost degradation rate relative to that with only conductive input (from 9.1 to 17.5 cm/year). McKenzie and Voss (2013) also report that conduction and advection have similar magnitude effects on permafrost thaw rates, though their analysis focused on taliks beneath lakes and groundwater exchanges were the source of (vertical) advection. Lateral flows as the source of advection similar to the ones modeled here were considered by de Grandpré et al. (2012), where advection contributed a significant amount of heat to thaw permafrost under a road bed, though the relative contribution of advection was not computed.

The assumption of a constant gradient in the simulations of a bog and a fen neglects the variability in this data. In the case that a talik connects two wetland features, this assumption is reasonable. Though there may be seasonal changes in pressure (especially during the freshet), there is enough water stored in each feature to sustain flow over the winter without large changes in gradient. However, a small isolated talik adjacent to a wetland (with a single connection) likely does not have the storage capacity to sustain flows over winter, so the impacts of advection would be less in these cases. Observed rates of permafrost degradation at the SCRS are slower in these cases.

To better understand the dependence of thaw rate on temperature and rate of advection, 42 simulations with consistent *stable* boundary and *talik* initial conditions were completed for a range of advective flow rates and incoming temperatures. Figures 8d and 8e show the change in permafrost degradation rate due to increasing mean advection temperature and hydraulic gradient. Permafrost degradation rate for each simulation was calculated as the slope of a linear fit to the maximum annual depth to permafrost over a 10-year simulation. The inflow temperature was sampled between  $T_{in} - 1^{\circ}\text{C}$  and  $T_{in} + 3^{\circ}\text{C}$ , where  $T_{in}$  is the mean daily inflow temperature representative of a bog which never drops below  $1.2^{\circ}\text{C}$ .

Thaw rates are comparably sensitive to changes in hydraulic gradient and advection temperature, where an increase in gradient or temperature leads to a clear increase in permafrost thaw rate, as may be expected from examining equation (3). Both relations are linear in the range unaffected by changes in hydraulic conductivity due to partial ice saturation. As seen in Figure 8e, at low-flow rates, pore ice formation limits the hydraulic conductivity, and thus, the impact of hydraulic gradient on thaw rate is suppressed (up to a gradient of approximately 0.005). In the field, this decrease in hydraulic conductivity may lead to a resulting increase in hydraulic gradient as water movement becomes limited, pushing advection out of this nonlinear, low-flow region. Increases in hydraulic gradient may also be expected during the freshet when ice and snow prevent overland flow and result in ponded water on the landscape, though many flow pathways would be clogged with frozen pore water. Such complicated interplay between partially frozen soils and groundwater flow is similarly documented in de Grandpré et al. (2012).

## 5. Synthesis

### 5.1. Drivers of Talik Formation

A comparison of Figures 4–6 indicate that soil moisture conditions and changes in SWE have effects of similar magnitude on the formation of taliks over the expected range of parameter values observed in the field. The magnitude of the resulting change in talik thickness is similar to that observed for a change in ground surface temperature of  $0.5^{\circ}\text{C}$ . This suggests that with projected climate warming in Northern Canada (Solomon et al., 2007), talik formation is likely regardless of changes in soil moisture and SWE regimes.

Model simulations indicate that small variability in forcing even over a single season can lead to permafrost degradation and talik formation. This sensitivity to perturbation is not unique to the SCRS, where the permafrost can be classified as ecosystem protected, as defined by Shur and Jorgenson (2007). Robinson and Moore (2000) describe how changes to the surface layer of peat due to wildfire can lead to permafrost degradation, but other disruptions to it such as an abnormally wet summer, the removal of a tree canopy, or anthropogenic compaction of the surface layer are also very likely to lead to talik formation (through the process shown in Figure 4).

Though soil moisture, ground heat flux, and SWE are thought to be the main drivers of talik formation, there were other factors that should receive attention. One such factor is the timing of the snow-covered period as a control on the refreeze process. Though not simulated here, it is anticipated that a prolonged delay

between the onset of freezing conditions and the arrival of substantial snowfall would result in enhanced refreeze depths as the absence of snow would not only increase the conductive heat transfer through the soil surface but also leave the bare surface exposed to convective heat transfer. Measurements and simulations by Zhang et al. (2007) confirm this, showing earlier and deeper refreeze in a year with late snow onset. This is observed in the field as the sloping edges of channel fens, which are scoured by wind in early winter generally exhibit refreeze about 10 cm deeper than other, more protected, areas in the landscape.

## 5.2. Talik Formation as a Tipping Point

Modeling results from section 4.3 demonstrate that once a talik is present in the soil column, only changes to soil moisture are able to initiate permafrost recovery in the studied discontinuous permafrost peatlands environment. The other cases including cooler mean annual surface temperatures and decreases in SWE (within ranges observed at the SCRS) did not lead to any talik thinning. Comparing results presented in sections 4.2 and 4.3 leads to the generalization that changes in mean annual temperature results in increased permafrost degradation rates once a talik is formed. Changes to soil moisture and SWE caused slower talik thickening after talik formation due to the increased soil column depth but did show more sensible heat storage.

Advection modeling tests (section 4.4) showed that lateral flow through a connected talik significantly increases thaw rates, which has been verified by field observations. Such flow pathways are permanently active year-round and can contribute significantly to permafrost thaw in a manner that is likely irreversible, since advection can only supply energy to frozen ground. McClymont et al. (2013) document advection as a dominant control on permafrost thaw, but in this work, as in others (e.g., Walvoord & Kurylyk, 2016), advection is the result of flows along the edges of peat plateaux, along channel fens, or in the moat of collapse scar bogs. Here it is proposed that advection through a talik connecting wetland features (i.e., a bog connected to a fen via a talik) would also lead to thermal erosion of permafrost at the top of a permafrost body. This has the potential for a much higher hydraulic gradient and subsequent flow rate than may be expected in a channel fen in this low-relief landscape (with a typical gradient of 0.0032 [Stone, 2018] as compared to a gradient of 0.01 measured between features connected by a talik), especially over winter when ice and snow-load can increase subsurface pressure in the landscape.

Given the drivers of talik formation and evolution identified above, the model was applied using observed field conditions to predict likely changes in permafrost in different parts of this landscape. These conditions are the *plateau* initial condition with *stable* boundary condition (Stable Plateau) and *talik* initial condition with *degrading* boundary conditions (degrading talik).

### 5.2.1. Stable Plateau

None of the 20 realizations of surface boundary conditions constructed using the seasonal autoregressive model of the *stable* condition discussed in section 3.3 with an initial water table at a depth of 0.5 m below the surface resulted in the formation of a talik in the 10 years modeled. The simulations did, however, show potential for active layer thickening, as reported in Shiklomanov et al. (2012). There was an increase in maximum thaw depth (with complete refreeze) of approximately 0.3 cm/year over the entire 10-year simulation, with the same average rate in only the last 5 years of simulation for the stable condition. Figure 9a shows the distribution of rates of permafrost degradation for this *stable* boundary condition on the left for the entire 10-year simulation (gray), and then only for the last 5 years of simulation (black). Agreement between these supports an appropriate selection of initial conditions. The small annual loss of permafrost in a 10-year simulation indicates that the current condition of peat plateaux results in permafrost degradation. Given long enough periods forced with these consistent boundary conditions, it is expected that the permafrost will begin to degrade, as discussed for this field site in Quinton et al. (2019). This is analogous to results found by Briggs et al. (2014) who show that though permafrost aggradation has been observed in draining lakes, this phenomenon is only transitional as the permafrost is an artifact of the groundwater regime and shading from shrubs, and it is expected to thaw within the decade.

At the SCRS there is clear evidence of degrading permafrost. Evidence of aggrading permafrost is sparse and unconfirmed, suggesting that permafrost formation may not be possible in the current climate unless significant dewatering of the landscape occurs. Though sections of permafrost peat plateaux appear stable, they are extremely vulnerable to change as the underlying permafrost is not in equilibrium with the current climate. Given the slow rate of permafrost degradation identified from models with the current boundary conditions, it is only a matter of time before this ecosystem-protected permafrost degrades even without

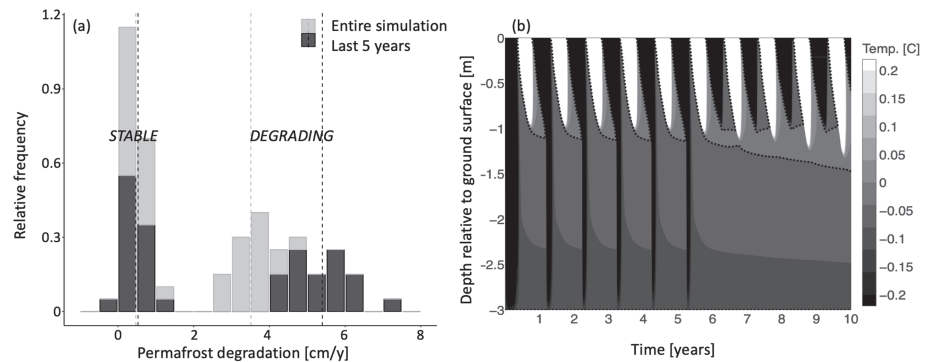


**Figure 9.** (a) Stacked relative frequency distribution of permafrost degradation rates modeled with *stable* boundary condition (left) and *degrading* condition (right). Vertical dashed lines indicate the mean permafrost degradation rate for the entire simulation (10 years) or for only the last 5 years of simulation. (b) Talik formation (for the *degrading* boundary condition) shown as a temperature contour plot. Note that the incomplete refreeze in the sixth winter initiates the formation of a talik, which then provides a previously absent pathway for advection.

the additional mechanisms discussed above. Using tree canopy as a proxy for permafrost (Carpino et al., 2018), aerial imagery from this study site was compared from 1947 to 2008, showing a  $38 \pm 8\%$  decrease in permafrost coverage (Quinton et al., 2011), indicating that this degradation is already underway. This is echoed in the findings of Kwong and Gan (1994) describing a northward moving southern limit of sporadic and discontinuous permafrost due to increases in mean annual temperature.

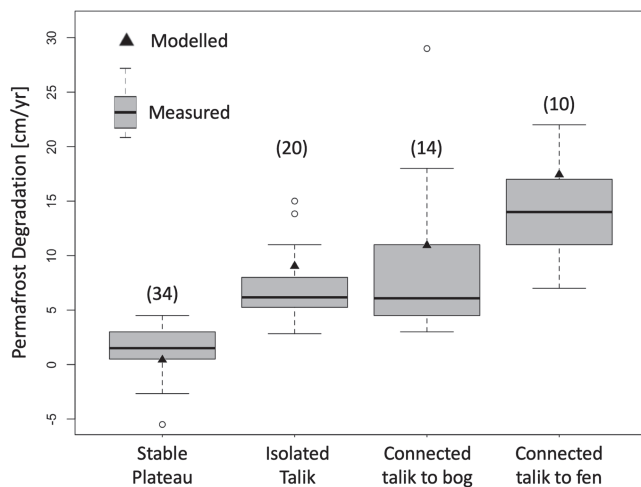
### 5.2.2. Expanding Talik

Figure 9 (a—*degrading*) shows the response of an initially talik-free system to the *degrading* boundary condition. The formation of a talik increases permafrost thaw rates while also increasing the variability in thaw rate. The variance in simulated thaw rates is significantly greater in the case with a talik for two possible reasons: (1) These simulations include the formation of the talik, as shown in Figure 9b, which is sensitive to changes in boundary conditions; and (2) The formation of a connected talik allows for advection, which is further modified by the presence of ice in the soil column affecting the permeability. It is not appropriate to compare the permafrost degradation rate in the stable case directly to the talik case as the boundary conditions in each scenario differ. The impact of talik formation on permafrost thaw can, however, be discussed by focusing only on the talik condition simulations.

An example of talik formation can be seen in Figure 9b. The first five winters of this simulation involve complete refreeze and subsequent cooling of the underlying permafrost. As soon as a talik is formed in year 6, the underlying permafrost remains near the measured freezing point depression and above the temperature at which the freezing function used in the model reaches residual unfrozen saturation. This simulation aptly demonstrates that permafrost degradation clearly accelerates once a talik forms, as can be seen to the right of Figure 9 (a—*degrading*). This is anticipated for three reasons: (1) the activation of an advective flow pathway, (2) a reversal of the temperature gradient, and (3) (in the case of field measurements) subsidence of the ground surface, resulting in a positive feedback leading to increased soil moisture.

The presence of a talik with a temperature at or above the zero-point depression alters the ground temperature profile such that the surface of a permafrost body always experiences a positive (or zero) temperature gradient (Connon et al., 2018). The permafrost at or below the freezing point depression is always colder than the overlaying thawed talik and consequently gains thermal energy year-round. This can be seen in Figure 1a, which shows the (colinear) maximum and minimum annual temperatures measured over a talik. The talik is apparent in the figure as the region (in gray) that never cools below the zero-point depression but is warmed in the summer. Below this region, the permafrost is essentially isothermal in the zero curtain, indicating that it is undergoing phase change and is unable to lose energy to the atmosphere. In combination with advection, this can lead to the overwinter permafrost thaw observed in the SCRS. One such connected talik feature connecting a bog and fen has exhibited 21 cm of thaw between August 2016 and May of 2017 and 13 cm of thaw between September 2017 and April of 2018.

In the field, the positive feedback of permafrost degradation after talik formation is furthered by an increase in soil moisture due to ground surface subsidence. As shown in section 4.2.1, this increase leads to slightly



**Figure 10.** Comparison of permafrost thaw rates in different portions of the landscape. Box and whisker plot shows spread in measured talik development data, while triangles show average modeled value for each type of talik. A total of 78 locations was measured semiannually over the course of 8 years to generate the permafrost degradation rate data. Note that points fall outside of 1.5 times the interquartile range, the upper bound of the whiskers.

enhanced thaw rates, but increased soil moisture also counteracts the only realistic modeled conditions able to promote permafrost recovery—an unsaturated soil column. More energy is able to reach the permafrost table both due to the increased thermal conductivity, as well as a thinning canopy as the black spruce (*Picea mariana*) suffer from water logging of their root networks (Quinton & Baltzer, 2013). The depressions formed allow for preferential accumulation of snow, which was shown to trigger permafrost thaw. In this sense, the formation of a talik can be seen as a tipping point leading to accelerated permafrost thaw rates with little chance of recovery.

### 5.3. Permafrost Degradation in the Landscape

Given the impacts of soil moisture, advection, and the existence of taliks on permafrost degradation rates, it is expected that the rates of permafrost degradation should differ across landscape features. Sjöberg et al. (2016) suggest that the relative importance of thaw mechanisms including conduction and vertical or lateral advection varies both seasonally and across different peatland landscape features. To better capture thaw in each part of the landscape, a final modeling experiment was undertaken. In this experiment, advection was forced with temperatures based on profiles observed in a bog and a fen at the SCRS, similar to the simulations used to generate Figures 8a–8c. Temperature boundary conditions were consistent with the stable condition for the plateau landscape type, while the three talik conditions (isolated, connected bog, and connected fen) used

the a boundary condition constructed using the autoregressive model constructed for the talik condition. Modeled thaw rates are compared to thaw measured as change in end-of-season depth to permafrost using a frost probe at different locations in the landscape. This comparison is shown in Figure 10, where field data were categorized according to the type of talik. Note that the high variance in measured thaw rates in connected taliks adjacent to fens and bogs is likely due to variations in flow rate and temperature at different monitoring locations. The modeled thaw rates for taliks assume a saturated soil column. This explains the slight overestimation of thaw rates in isolated taliks, which are generally wetter than the surrounding stable plateau, but are rarely completely saturated in the field. Permafrost degradation is incrementally faster as advection rates and temperatures increase in bogs and fens, as demonstrated in Figure 8.

The slow but positive thaw rate observed on a “stable” plateau is indicative of a system in disequilibrium with the climate. The gradual permafrost loss either as active layer thickening or as talik formation points toward an eventual near-complete loss of permafrost from the system. Once a talik is formed, the rate of permafrost degradation is notably more rapid due to the combined effects of higher thermal conductivity, advection, canopy degradation, thermal storage in taliks, and ground surface subsidence.

At the landscape scale, permafrost loss is likely to emanate outward from existing wetland features, especially fens that have higher flow rates and temperatures, while preferentially forming the hydrologic connections between wetlands where the hydraulic gradient is greatest, as documented by Connon et al. (2015). Not only will the edges of permafrost cored peat plateaux be eroded, but depressions are likely to grow into isolated taliks, which will expand and interlink, leaving small isolated hummocks of permafrost as described in Quinton et al. (2018). These isolated permafrost features are documented in the sporadic permafrost region by Woo (2012).

The long-term evolution of discontinuous permafrost is complex and influenced by additional influences not included in the boundary conditions used here; hence, the simulation duration was limited to a decade. Such influences include gradual wetting of the soil profile due to subsidence, increase in surface temperature because of canopy loss, increased snow accumulation due to depression formation, and lateral flow rates and inflow temperatures that may vary based on upstream conditions. Under these more complete conditions, long-term simulations may be more meaningful, but it is likely that the positive feedbacks associated with talik-influenced permafrost thaw presented here would still play a critical role. Further work is needed to better quantify the role of isolated and connected taliks at a longer time scale, and it is anticipated that

multidimensional modeling may be necessary to inform a more complete understanding of talik influence on long-term permafrost evolution.

## 6. Conclusion

This study used a combination of extensive field data and 1-D modeling to investigate the formation of isolated taliks beneath the active layer. A freeze-thaw model was developed that reproduces temperature data and refreeze depths in discontinuous permafrost peatlands. This model was used to provide a rigorous evaluation of the controls on isolated talik formation, which is prevalent in discontinuous permafrost environments and can be driven by soil moisture, snow accumulation, and/or seasonal temperature trends. Soil moisture, ground heat flux, snow cover, and advection were all found to affect the formation of taliks in different contexts. It was deemed difficult to identify which factor is dominant as they often occur simultaneously and are interdependent. However, wet conditions, deep snow, and warmer soil surface temperatures were found to increase the probability and rate of isolated talik formation. Isolated talik formation was shown to be a tipping point in permafrost degradation, leading to accelerated permafrost thaw, which is unlikely to recover once the talik is formed. Once a talik is formed, permafrost degradation can be accelerated by subsurface flows through the talik (especially if it forms a pathway between wetland features), increased soil moisture, increased ground heat flux, and snow accumulation due to a critical lack of energy loss from the permafrost to the atmosphere overwinter. Only unsaturated conditions (highly unlikely in permafrost degrading within a wetland system) were found to lead to permafrost recovery, resulting in accelerated and potentially irreversible permafrost thaw in this environment. It may therefore be pertinent to consider talik formation in models of other permafrost environments, especially at larger scales where these processes are often neglected, but may lead to significantly different permafrost conditions.

## Acknowledgments

We greatly appreciate the support from Gabriel Hould Gosselin, John Coughlin, and Dirk J. Friesen in data collection and fieldwork, as well as Kristine Haynes in data processing. We wish to thank the Liidlii Kue First Nation and the Jean Marie River First Nation for their continued support of the SCRS. We would also like to thank Wayne and Lynn MacKay for providing logistical support to the SCRS. We acknowledge the generous support of the Government of the Northwest Territories through their partnership agreement with Wilfrid Laurier University and of the Cold Regions Research Centre. This work is completed for the Consortium for Permafrost Ecosystems in Transition (CPET) project, funded by NSERC CRD and Polar Knowledge Canada. We also wish to thank NSERC and Northern Scientific Training Program for providing additional funding for this project. All data presented in this article can be found in the Wilfrid Laurier university Library archive (<https://doi.org/10.5683/SP2/BTRLHO>).

## References

- Atchley, A. L., Coon, E. T., Painter, S. L., Harp, D. R., & Wilson, C. (2016). Influences and interactions of inundation, peat, and snow on active layer thickness. *Geophysical Research Letters*, 43, 5116–5123. <https://doi.org/10.1002/2016GL068550>
- Atchley, A. L., Painter, S. L., Harp, D. R., Coon, E. T., Liljedahl, A. K., & Romanovsky, V. E. (2015). Using field observations to inform thermal hydrology models of permafrost dynamics with ATS (v0.83). *Geoscientific Model Development*, 8, 2701–2722.
- Baltzer, J. L., Veness, T., Chasmer, L. E., Sniderhan, A. E., & Quinton, W. L. (2014). Forests on thawing permafrost: Fragmentation, edge effects, and net forest loss. *Global Change Biology*, 20, 824–834.
- Bonnaveure, P., & Lamoureux, S. (2013). The active layer: A conceptual review of monitoring, modelling techniques and changes in a warming climate. *Progress in Physical Geography*, 37, 352–376.
- Briggs, M. A., Walvoord, M. A., McKenzie, J. M., Voss, C. L., Day-Lewis, F. D., & Lane, J. W. (2014). New permafrost is forming around shrinking arctic lakes, but will it last? *Geophysical Research Letters*, 41, 1585–1592. <https://doi.org/10.1002/2014GL059251>
- Brown, D. R. N., Jorgenson, M. T., Douglas, T. A., Romanovsky, V. E., Kielland, K., Hiemstra, C., et al. (2015). Interactive effects of wildfire and climate on permafrost degradation in alaskan lowland forests. *Journal of Geophysical Research: Biogeosciences*, 120, 1619–1637. <https://doi.org/10.1002/2015JG003033>
- Burn, C. (1998). The active layer: Two contrasting definitions. *Permafrost and Periglacial Processes*, 9, 411–416.
- Carpino, O. A., Berg, A. A., Quinton, W. L., & Adams, J. R. (2018). Climate change and permafrost thaw-induced boreal forest loss in northwestern Canada. *Environmental Research Letters*, 13, 084018.
- Celia, M. A., Bouloutas, E. T., & Zarba, R. L. (1990). A general mass-conservative numerical solution for the unsaturated flow equation. *Water Resources Research*, 26, 1483–1496. <https://doi.org/10.1029/WR026i007p01483>
- Chasmer, L., Quinton, W. L., Hopkinson, C., Petrone, R., & Whittington, P. (2011). Vegetation canopy and radiation controls on permafrost plateau evolution within the discontinuous permafrost zone, Northwest Territories, Canada. *Permafrost and Periglacial Processes*, 22, 199–213.
- Connon, R. F., Devoie, É., Hayashi, M., Veness, T., & Quinton, W. L. (2018). The influence of shallow taliks on permafrost thaw and active layer dynamics in subarctic Canada. *Journal of Geophysical Research: Earth Surface*, 123, 281–297. <https://doi.org/10.1002/2017JF004469>
- Connon, R. F., Quinton, W. L., Crag, J. R., Hanisch, J., & Sonnentag, O. (2015). The hydrology of interconnected bog complexes in discontinuous permafrost terrains. *Hydrological Processes*, 29, 3831–3847.
- Daanen, R. P., Misra, D., Epstein, H., Walker, D., & Romanovsky, V. (2008). Simulating nonsorted circle development in arctic tundra ecosystems. *Journal of Geophysical Research*, 113, G03S06. <https://doi.org/10.1029/2008JG000682>
- de Grandpré, I., Fortier, D., & Stephani, E. (2012). Degradation of permafrost beneath a road embankment enhanced by heat advected in groundwater. *Canadian Journal of Earth Sciences*, 49, 953–962.
- Endrizzi, S., Gruber, S., Dall'Amico, M., & Rigon, R. (2014). Geotop 2.0: Simulating the combined energy and water balance at and below the land surface accounting for soil freezing, snow cover and terrain effects. *Geoscientific Model Development*, 7, 2831–2857.
- Evans, S. G., & Ge, S. (2017). Contrasting hydrogeologic responses to warming in permafrost and seasonally frozen ground hillslopes. *Geophysical Research Letters*, 44, 1803–1813. <https://doi.org/10.1002/2016GL072009>
- Fisher, J. P., Estop-Aragón, C., Thierry, A., Charman, D. J., Wolfe, S. A., Hartley, I. P., et al. (2016). The influence of vegetation and soil characteristics on active-layer thickness of permafrost soils in boreal forest. *Global Change Biology*, 22, 3127–3140.
- Frampton, A., Painter, S. L., & Destouni, G. (2012). Permafrost degradation and subsurface-flow changes caused by surface warming trends. *Hydrogeology of Cold Regions*, 21, 271–280.
- Gordon, J., Quinton, W. L., Branfireun, B. A., & Olefeldt, D. (2016). Mercury and methylmercury biogeochemistry in a thawing permafrost wetland complex, Northwest Territories, Canada. *Hydrological Processes*, 30, 3627–3638.

- Grant, R. F., Mekonnen, Z. A., Riley, W. J., Wainwright, H. M., Graham, D., & Torn, M. S. (2017). Mathematical modelling of arctic polygonal tundra with ecosys: 1. Microtopography determines how active layer depths respond to changes in temperature and precipitation. *Journal of Geophysical Research: Biogeosciences*, 122, 3161–3173. <https://doi.org/10.1002/2017JG004035>
- Grosse, G., Goetz, S., McGuire, A. D., Romanovsky, V. E., & Schuur, E. A. (2016). Review and synthesis: Changing permafrost in a warming world and feedbacks to the earth system. *Environmental Research Letters*, 11, 040201.
- Harlan, R. L. (1973). Analysis of coupled heat-fluid transport in partially frozen soil. *Water Resources Research*, 9, 1314–1323.
- Hayashi, M., Quinton, W. L., Goeller, N., & Wright, N. (2007). A simple heat-conduction method for simulating the frost-table depth in hydrological models. *Hydrological Processes*, 21, 2610–2622.
- Hinzman, L. D., Goering, D. J., & Kane, D. L. (1998). A distributed thermal model for calculating soil temperature profiles and depth of thaw in permafrost regions. *Journal of Geophysical Research*, 103, 28,975–28,991.
- Hipel, K. W., & McLeod, A. I. (1994). *Time series modelling of water resources and environmental systems*. Amsterdam: Elsevier Science.
- Jafarov, E. E., Coon, E. T., Harp, D. R., Painter, C. J. W. S. L., Atchley, A. L., & Romanovsky, V. E. (2018). Modeling the role of preferential snow accumulation in through talik development and hillslope groundwater flow in a transitional permafrost landscape. *Environmental Research Letters*, 13, 105006.
- Jorgenson, M. T., Romanovsky, V., Harden, J., Yuri Shur, J. O., Schuur, E. A. G., Kanevskiy, M., & Marchenko, S. (2010). Resilience and vulnerability of permafrost to climate change. *Canadian Journal of Forest Research*, 40, 1219–1236.
- Karra, S., Painter, S. L., & Lichtner, P. C. (2014). Three-phase numerical model for subsurface hydrology in permafrost-affected regions (pflotran-ice v1.0). *The Cryosphere*, 8, 1935–1950.
- Krogh, S. A., Pomeroy, J. W., & Marsh, P. (2017). Diagnosis of the hydrology of a small arctic basin at the tundra-taiga transition using a physically based hydrologic model. *Journal of Hydrology*, 550, 685–703.
- Kurylyk, B. L. (2013). The mathematical representation of freezing and thawing processes in variably-saturated, non-deformable soils. *Advances in Water Resources*, 60, 160–177.
- Kurylyk, B. L., Hayashi, M., Quinton, W. L., McKenzie, J. M., & Voss, C. L. (2016). Influence of vertical and lateral heat transfer on permafrost thaw, peatland landscape transition, and groundwater flow. *Water Resources Research*, 52, 1286–1305. <https://doi.org/10.1002/2015WR018057>
- Kurylyk, B. L., McKenzie, J. M., MacQuarrie, K. T., & Voss, C. I. (2014). Analytical solutions for benchmarking cold regions subsurface water flow and energy transport models: One-dimensional soil thaw with conduction and advection. *Advances in Water Resources*, 70, 172–184.
- Kwong, Y. T. J., & Gan, T. Y. (1994). Northward migration of permafrost along the Mackenzie highway and climatic warming. *Climatic Change*, 26, 399–419.
- Langford, J. E., Schincariol, R., Nagare, R., Quinton, W. L., & Mohammed, A. (2019). Transient and transition factors in modeling permafrost thaw and groundwater flow. *Groundwater*, 1–11. <https://doi.org/10.1111/gwat.12903>
- McClymont, A. F., Hayashi, M., Bentley, L. R., & Christensen, B. S. (2013). Geophysical imaging and thermal modeling of subsurface morphology and thaw evolution of discontinuous permafrost. *Journal of Geophysical Research: Earth Surface*, 118, 1826–1837. <https://doi.org/10.1002/jgrf.20114>
- McGuire, A. D., Koven, C., Lawrence, D. M., Clein, J. S., Xia, J., Beer, C., et al. (2016). Variability in the sensitivity among model simulations of permafrost and carbon dynamics in the permafrost region between 1960 and 2009. *Global Biogeochemical Cycles*, 30, 1015–1037. <https://doi.org/10.1002/2016GB005405>
- McKenzie, J. M., & Siegel, D. (2007). Groundwater flow with energy transport and water-ice phase change: Numerical simulations, benchmarks, and application to freezing in peat bogs. *Advances in Water Resources*, 30, 966–983.
- McKenzie, J. M., & Voss, C. L. (2013). Permafrost thaw in a nested groundwater-flow system. *Hydrogeology of Cold Regions*, 21, 299–316.
- Nickolsky, D. J., Romanovsky, V. E., Panda, S. K., Marchenko, S., & Muskett, R. R. (2016). Applicability of the ecosystem type approach to model permafrost dynamics across the alaska north slope. *Journal of Geophysical Research: Earth Surface*, 122, 50–75. <https://doi.org/10.1002/2016JF003852>
- O'Donnell, J. A., Romanovsky, V. E., Harden, J. W., & McGuire, A. D. (2009). The effect of moisture content on the thermal conductivity of moss and organic soil horizons from black spruce ecosystems in interior alaska. *Soil Science*, 174, 646–651.
- Putkonen, J. (1998). Soil thermal processes and heat transfer processes near ny-ålesund, northwestern Spitsbergen, Svalbard. *Polar Research*, 17, 165–179.
- Quinton, W. L., & Baltzer, J. L. (2013). The active-layer hydrology of a peat plateau with thawing permafrost (Scotty Creek, Canada). *Hydrogeology Journal*, 21, 201–220.
- Quinton, W. L., Berg, A. A., Braverman, M., Carpino, O. A., Chasmer, L., Connon, R. F., et al. (2019). A synthesis of three decades of ecohydrological research at Scotty Creek, NWT, Canada. *Hydrology and Earth System Sciences*, 23, 2015–2039.
- Quinton, W. L., Berg, A. A., Carpino, O. A., Connon, R. F., Crag, J. R., Devoie, É., & Johnson, E. (2018). Toward understanding the trajectory of hydrological change in the southern Taiga Plains, northeastern British Columbia and southwestern Northwest Territories. Geoscience BC Summary of Activities 2017:Energy.
- Quinton, W. L., Hayashi, M., & Carey, S. K. (2008). Peat hydraulic conductivity in cold regions and its relation to pore size and geometry. *Hydrological Processes*, 22, 2829–2837.
- Quinton, W. L., Hayashi, M., & Chasmer, L. E. (2009). Peatland hydrology of discontinuous permafrost in the Northwest Territories: Overview and synthesis. *Canadian Water Resources Journal*, 34, 311–328.
- Quinton, W. L., Hayashi, M., & Chasmer, L. E. (2011). Permafrost-thaw-induced land-cover change in the Canadian Subarctic: Implications for water resources. *Hydrological Processes*, 25, 152–158.
- Rawlins, M. A., Nickolsky, D. J., McDonald, K. C., & Romanovsky, V. E. (2013). Simulating soil freeze/thaw dynamics with an improved pan-arctic water balance model. *Journal of Advances in Modelling Earth Systems*, 5, 659–675. <https://doi.org/10.1002/jame.20045>
- Robinson, S. D., & Moore, T. R. (2000). The influence of permafrost and fire upon carbon accumulation in high boreal peatlands, Northwest Territories, Canada. *Arctic, Antarctic and Alpine Research*, 32, 155–166.
- Rowland, J. C., Jones, C. E., Altman, G., Bryan, R., Crosby, B. T., Greenaert, G. L., et al. (2010). Arctic landscapes in transition: Responses to thawing permafrost. *EOS Transactions, Geophysical Union*, 91, 229–236.
- Schaefer, K., Zhang, T., Slater, A. G., Lu, L., Etringer, A., & Baker, I. (2009). Improving simulated soil temperatures and soil freeze/thaw at high-latitude regions in the Simple Biosphere/Carnegie-Ames-Stanford Approach model. *Journal of Geophysical Research*, 114, F02021. <https://doi.org/10.1029/2008JF001125>
- Semenova, O., Lebedeva, L., & Vinogradov, Y. (2013). Simulation of subsurface heat and water dynamics, and runoff generation in mountainous permafrost conditions, in the Upper Kolyma River Basin, Russia. *Hydrogeology of Cold Regions*, 21, 107–119.

- Shiklomanov, N. I., Streletskiy, D. A., & Nelson, F. E. (2012). Northern Hemisphere component of the global Circumpolar Active Layer Monitoring (CALM) program. In *Proceedings of the Tenth International Conference on Permafrost*.
- Shook, K., Pomeroy, J. W., & van der Kamp, G. (2015). The transformation of frequency distributions of winter precipitation to spring stream flow probabilities in cold regions; Case studies from the canadian prairies. *Journal of Hydrology*, 521, 395–409.
- Shur, Y. L., & Jorgenson, M. T. (2007). Patterns of permafrost formation and degradation in relation to climate and ecosystems. *Permafrost and Periglacial Processes*, 1
- Sjöberg, Y., Coon, E. T., Sannel, A. B. K., Pannetier, R., Harp, D. R., Frampton, A., et al. (2016). Thermal effects of groundwater flow through subarctic fens: A case study based on field observations and numerical modeling. *Water Resources Research*, 52, 1591–1606. <https://doi.org/10.1002/2015WR017571>
- Solomon, S., Qin, D., Manning, M., Averyt, K., & Marquis, M. (2007). *Climate change 2007—The physical science basis: Working Group I Contribution to the Fourth Assessment Report of the IPCC*. Cambridge: Cambridge University Press.
- Stendel, M., & Christiansen, H. (2002). Impact of global warming on permafrost in a coupled GCM. *Geophysical Research Letters*, 29(13), 1632. <https://doi.org/10.1029/2001GL014345>
- Stone, L. E. (2018). The role of channel fens in permafrost degradation induced changes in peatland discharge at Scotty Creek, NWT (Unpublished master's thesis), Wilfrid Laurier University.
- van Genuchten, M. T. (1980). A closed-form equation for predicting the hydraulic conductivity of unsaturated soils. *Soil Science Society*, 44, 892–898.
- Walvoord, M. A., & Kurylyk, B. L. (2016). Hydrologic impacts of thawing permafrost—A review. *Vadose Zone Journal*, 15, vzj2016.01.0010.
- Walvoord, M. A., Voss, C. L., Ebel, B. A., & Minsley, B. J. (2019). Development of perennal thaw zones in boreal hillslopes enhances potential mobilization of permafrost carbon. *Environmental Research Letters*, 14, 015003.
- Woo, M. (2012). *Permafrost hydrology*. Verlag Berlin Heidelberg: Springer.
- Woo, M., Arain, M. A., Mollinga, M., & Yi, S. (2004). A two-directional freeze and thaw algorithm for hydrologic and land surface modelling. *Geophysical Research Letters*, 31, L12501. <https://doi.org/10.1029/2004GL019475>
- Yi, S., Wischniewski, K., Langer, M., Muster, S., & Boike, J. (2014). Freeze/thaw processes in complex permafrost landscapes of northern siberia simulated using the TEM ecosystem model: Impact of thermokarst ponds and lakes. *Geoscientific Model Development*, 7, 1671–1689.
- Zhang, Y., Chen, W., & Cihlar, J. (2003). A process-based model for quantifying the impact of climate change on permafrost thermal regimes. *Journal of Geophysical Research*, 108(D22), 4695. <https://doi.org/10.1029/2002JD003354>
- Zhang, Y., Chen, W., & Riseborough, D. W. (2008). Disequilibrium response of permafrost thaw to climate warming in Canada over 1850–2100. *Geophysical Research Letters*, 35, L02502. <https://doi.org/10.1029/2007GL032117>
- Zhang, Y., Wang, S., Barr, A. G., & Black, T. (2007). Impact of snow cover on soil temperature and its simulation in a boreal aspen forest. *Cold Regions Science and Technology*, 52, 355–370.
- Zhao, L., Wu, Q., Marchenko, S., & Sharkhuu, N. (2010). Thermal state of permafrost and active layer in central Asia during the international polar year. *Permafrost and Periglacial Processes*, 21, 198–207.